

Early Pliocene vegetation and hydrology changes in western equatorial South America

Friederike Grimmer¹, Lydie Dupont¹, Frank Lamy², Gerlinde Jung¹, Catalina González³, Gerold Wefer¹

¹MARUM – Center for Marine Environmental Sciences, University of Bremen, Leobener Str. 8, 28359 Bremen, Germany

²Alfred-Wegener-Institute for Polar and Marine Research, Am Handelshafen 12, 27570 Bremerhaven, Germany

³Department of Biological Sciences, Universidad de los Andes, Cra. 1 #18a-12, Bogotá, Colombia

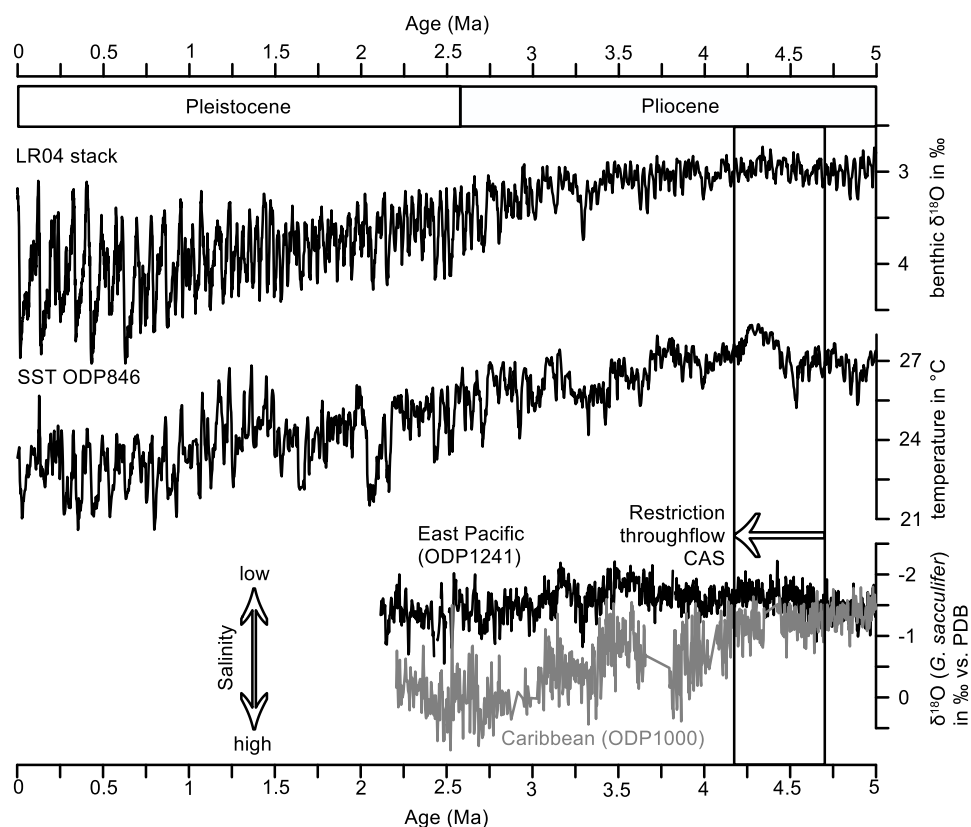
Correspondence to: Friederike Grimmer (fgrimmer@marum.de)

Abstract. During the early Pliocene, two major tectonic events triggered a profound reorganization of ocean and atmospheric circulation in the Eastern Equatorial Pacific (EEP), the Caribbean Sea, and on adjacent land masses: the progressive closure of the Central American Seaway (CAS) and the uplift of the northern Andes. These affected amongst others the mean latitudinal position of the Intertropical Convergence Zone (ITCZ). The direction of an ITCZ shift however is still debated, as numeric modelling results and paleoceanographic data indicate shifts in opposite directions. To provide new insights into this debate, an independent hydrological record of western equatorial South America was generated. Vegetation and climate of this area were reconstructed by pollen analysis of 46 samples from marine sediments of ODP Hole 1239A from the EEP comprising the interval between 4.7 and 4.2 Ma. The study site is sensitive to latitudinal ITCZ shifts insofar as a southward (northward) shift would result in increased (decreased) precipitation over Ecuador. The presented pollen record comprises representatives from five ecological groups: lowland rainforest, lower montane forest, upper montane forest, páramo, and broad range taxa. A broad tropical rainforest coverage persisted in the study area throughout the early Pliocene, without significant open vegetation beyond the páramo. Between 4.7 and 4.42 Ma, humidity increases, reaching its peak around 4.42 Ma, and slightly decreasing again afterwards. The stable, permanently humid conditions are rather in agreement with paleoceanographic data indicating a southward shift of the ITCZ, possibly in response to CAS closure. The presence of páramo vegetation indicates that the Ecuadorian Andes had already reached considerable elevation by the early Pliocene. Future studies could extend the hydrological record of the region further back into the late Miocene to see if a more profound atmospheric response to tectonic changes occurred earlier.

1 Introduction

The progressive closure of the Central American Seaway (CAS) and the uplift of the northern Andes profoundly reorganized early Pliocene ocean and atmospheric circulation in the Eastern Equatorial Pacific (EEP). The formation of the Isthmus of Panama, and especially the precise temporal constraints of the closure of the Panama Strait, have been subject of numerous studies (Bartoli et al., 2005; Groeneveld et al., 2014; Hoorn and Flantua, 2015; Montes et al., 2015; Steph, 2005). A recent review based on geological, paleontological, and molecular records narrowed the formation *sensu stricto* down to 2.8 Ma (O’Dea et al., 2016). Temporal constraints on the restriction of the surface water flow through the gateway were established by salinity reconstructions on both sides of the Isthmus (Steph et al., 2006b, Fig. 1). The salinities first start to diverge around 4.5 Ma. A major step in the seaway closure between 4.7 and 4.2 Ma was also assumed based on the comparison of mass accumulation rates of the carbonate sand-fraction in the Caribbean Sea and the EEP (Haug and Tiedemann, 1998). The closure of the Central American Seaway has been associated with the development of the EEP cold tongue (EEP CT), strengthened upwelling in the EEP, the shoaling of the thermocline, and a mean latitudinal shift of the Intertropical Convergence Zone (ITCZ; (Steph, 2005; Steph et al., 2006a; Steph et al., 2006b; Steph et al., 2010). The direction of a potential shift of the ITCZ is still debated because of a discrepancy between paleoclimate reconstructions based on proxy data and numerical modelling results.

40 For the late Miocene, a northernmost paleoposition of the ITCZ at about 10–12°N has been proposed (Flohn, 1981; Hovan,
 41 1995). Subsequently, a southward shift towards 5°N paleolatitude between 5 and 4 Ma is indicated by eolian grain-size
 42 distributions in the eastern tropical Pacific (Hovan, 1995). Billups et al. (1999) provide additional evidence for a southward
 43 shift of the ITCZ between 4.4 and 4.3 Ma. Hence, most proxy data agree about a southward ITCZ shift during the early
 44 Pliocene. On the contrary, results from numerical modelling suggest a northward shift of the ITCZ in response to CAS closure
 45 (Steph et al., 2006b) and Andean uplift (Feng and Poulsen, 2014; Takahashi and Battisti, 2007).
 46 An independent record of the terrestrial hydrology for the early Pliocene from a study site that is sensitive to latitudinal ITCZ
 47 shifts could provide new insights to this debate. Schneider et al. (2014) also stress the need of reconstructions of the ITCZ in
 48 the early and mid-Pliocene in order to understand how competing effects like an ice-free northern hemisphere and a weak EEP
 49 CT balanced, and to reduce uncertainties of predictions. Even though changes of ocean–atmosphere linkages related to ENSO
 50 (El Niño Southern Oscillation) and ITCZ shifts strongly impact continental precipitation in western equatorial South America,
 51 most studies so far have focused on paleoceanographic features such as sea-surface temperatures and ocean stratification.



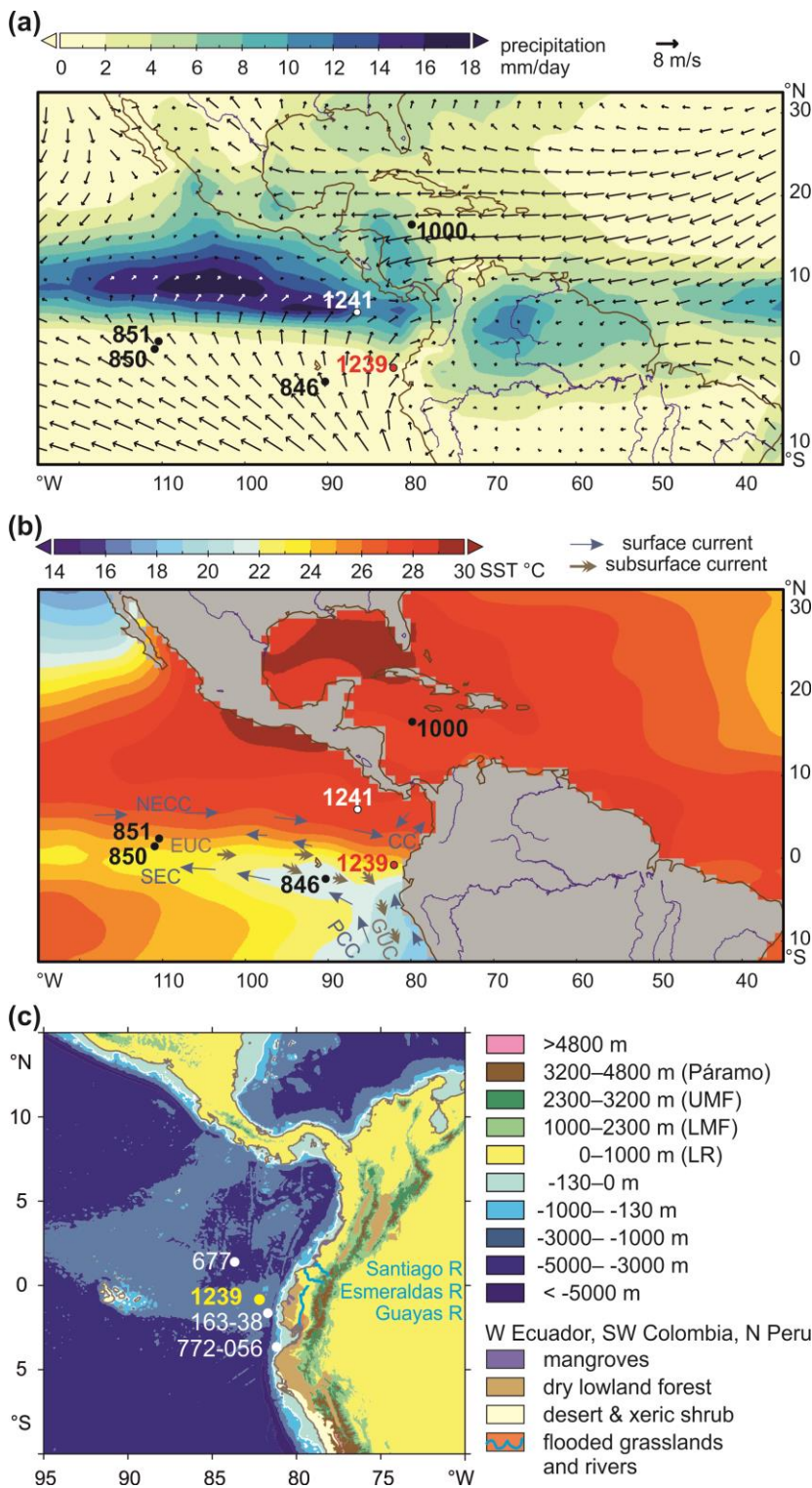
52
 53 **Figure 1.** LR04 global stack of benthic $\delta^{18}\text{O}$ reflecting changes in global ice volume and temperature (Lisiecki and Raymo, 2005).
 54 UK_{37} sea-surface temperatures (SST) of ODP Site 846 in the Equatorial Pacific Cold Tongue (Lawrence et al., 2006). $\delta^{18}\text{O}$ of the
 55 planktonic foraminifer *G. sacculifer* from ODP Site 1000 in the Caribbean and ODP Site 1241 in the East Pacific (Haug et al., 2001;
 56 Steph, 2005; Steph et al., 2006a), reflecting changes in sea-surface salinity (see Fig. 2 for location of ODP Sites). The box represents
 57 the time window analyzed in this study.

58
 59 The second major tectonic process is the uplift of the northern Andes which strongly altered atmospheric circulation patterns
 60 over South America. Three major deformation phases include fan building in the lower Eocene to early Oligocene,
 61 compression of Oligocene deposits in the Miocene and Pliocene, and refolding during Pliocene to recent times (Corredor,
 62 2003). While the uplift of the Central Andes is well investigated, only few studies deal with the timing of uplift of the northern
 63 Andes. Coltorti and Ollier (2000), based on geomorphologic data, conclude that the uplift of the Ecuadorian Andes started in
 64 the early Pliocene and continued until the Pleistocene. More recent apatite fission track data indicate that the western Andean
 65 Cordillera of Ecuador was rapidly exhumed during the late Miocene (13–9 Ma) (Spikings et al., 2005). Uplift estimates for the
 66 Central Andes suggest that the Altiplano had reached less than half of its modern elevation by 10 Ma, with uplift rates

67 increasing from 0.1 mm/yr in the early and middle Miocene to 0.2–0.3 mm/yr to present. For the Eastern Cordillera of
68 Colombia, elevations of less than 40% of the modern values are estimated for the early Pliocene, then increasing rapidly at
69 rates of 0.5–3 mm/yr until modern elevations were reached around 2.7 Ma (Gregory-Wodzicki, 2000). Both the tectonic events
70 and the closure of the Central American Seaway are assumed to have had a large impact on ocean and atmospheric circulation
71 in the eastern Pacific, the Caribbean and on adjacent land masses. Therefore, the reconstruction of continental climate,
72 especially hydrology, will contribute to our understanding of climatic changes in this highly complex area.

73 To better understand the early Pliocene vegetation and hydrology of western equatorial South America we studied pollen and
74 spores from the early Pliocene section (4.7–4.2 Ma) of the marine sediment record at ODP Site 1239 and compared this record
75 to Holocene samples from the same Site. In addition, we use elemental ratios to estimate variations in fluvial terrestrial input
76 (Ríncon-Martínez et al. 2010). While other palynological studies of the region have been conducted for the mid-Pliocene to
77 Holocene (González et al., 2006; Hooghiemstra, 1984; Seilles et al., 2016), only a few palynological records for the early
78 Pliocene exist (Wijninga and Kuhry, 1990; Wijninga, 1996). The record contributes to elucidate how vegetation and climate
79 in this area responded to changes in atmospheric and oceanic circulation, possibly induced by the closure of the Central
80 American Seaway and the uplift of the northern Andes. Therefore the main objectives of the study are firstly, to investigate
81 long-term vegetation and climatic changes, focusing on hydrology, in western equatorial South America and, secondly, to
82 interpret these changes in relation to climate phenomena influencing the hydrology of the region, especially the mean
83 latitudinal position of the ITCZ and variability related to ENSO. These objectives are approached by the following research
84 questions: 1) What floral and vegetation changes took place in the coastal plain of western equatorial South America and the
85 Ecuadorian Andes from 4.7 to 4.2 Ma? 2) What are the climatic implications of the vegetation change, especially in terms of
86 hydrology? 3) What are the implications for Andean uplift, especially regarding the development of the high Andean páramo
87 vegetation?

88
89



90

91

92

93

94

95

96

97

98

99

100

101

102

103

104

105

Figure 2. Modern climate (boreal summer) and vegetation and core site positions of ODP Sites 677, 846, 850, 851, 1000, 1239, 1241, Trident core TR163-38, and M772-056 mentioned in the text. A. 1981-2010 AD long-term monthly July precipitation in mm/day (CPC Merged Analysis of Precipitation) and .995 sigma level (near surface) wind field (NCEP). July is the middle of the rainy season in northern South America, when the ITCZ is at its northern boreal summer position. Salinity estimates for the Caribbean indicate a position of the ITCZ further north during the Pliocene. Direction of wind is not favorable for wind transport of pollen and spores to ODP Site 1239. B. Long-term monthly July sea-surface temperatures (NODC), surface and subsurface currents of the eastern equatorial Pacific (Mix et al. 2003). NECC, North Equatorial Countercurrent; SEC, South Equatorial Current; PCC, Peru-Chile Current (continuation of the Humboldt Current); CC, Coastal Current; EUC, Equatorial Undercurrent; GUC, Gunther Undercurrent. C. Contours, bathymetry (ETOPO1), main rivers in Ecuador, and vegetation. Transport of pollen and spores in the ocean over the Peru-Chile Trench, which is very narrow east of the Carnegie Ridge, probably takes place in nepheloid layers. Páramo vegetation is found between 3200 and 4800 m, upper montane Andean forest (UMF) grows between 1000 and 2300 m, sub-Andean lower montane forest (LMF) between 1000 and 2300 m, and lowland forest (LR) below 1000m. The distribution of desert and xeric shrubs in northern Peru, drier broad-leaved forest, flooded grasslands, and mangroves in Ecuador and Colombia is denoted in different colors (see legend, WWF). Source areas of pollen and spores in sediments of ODP Site 1239 are sought in western Ecuador, northwestern Peru, and southwestern Colombia (see text). Abbreviated web sources and retrieval dates are listed under references.

107 1.1 Modern setting

108 1.1.1 Climate and ocean circulation

109 The climate of western equatorial South America is complex and heterogeneous, as it is not only controlled by large-scale
 110 tropical climate phenomena such as the ITCZ and ENSO, but is also strongly influenced by small-scale climate patterns caused
 111 by the diverse Andean topography (Marchant et al., 2001; Niemann et al., 2010). The annual cycle of precipitation in
 112 northwestern South America is controlled by insolation changes. During boreal summer when insolation is strongest in the
 113 northern hemisphere, the ITCZ is located at its northernmost position around 9°–10° N (Vuille et al., 2000). Approaching
 114 austral summer, the ITCZ moves southward across the equator. Within the range of the ITCZ, annual precipitation patterns are
 115 generally characterized by two minima and two maxima. The coastal areas of southern Ecuador where the ITCZ has its
 116 southernmost excursion show an annual precipitation pattern with one maximum during austral summer and a pronounced dry
 117 season during austral winter (Bendix and Lauer, 1992).

118 This general circulation pattern is modified by ENSO at interannual time-scales. During warm El Niño events, the lowlands
 119 of Ecuador experience abundant precipitation whereas the northwestern Ecuadorian Andes experience drought (Vuille et al.,
 120 2000). Regional climate patterns are also modified by the topography of the Andes which pose an effective barrier for the
 121 large-scale atmospheric circulation. While precipitation patterns east of the Andes are driven by moisture-laden easterly trade
 122 winds originating over the tropical Atlantic and the Amazon basin, the coastal areas and the western Andean slopes are
 123 dominated by air masses originating in the Pacific (Vuille et al., 2000, Fig. 2). The warm annual El Niño current which flows
 124 southward along the Colombian Pacific coast warms the air masses along the coast. This moist air brings over 6000 mm yearly
 125 precipitation to the northern coastal plain. In contrast, the coastal areas of southernmost Ecuador and northern Peru are under
 126 the influence of the Peru-Chile Current, which is a continuation of the cold Humboldt Current transporting cold and nutrient
 127 rich waters and giving rise to a long strip of coastal desert (Balslev, 1988). The westwards flow of the cold surface waters of
 128 the EEP CT to the western Pacific via the South Equatorial Current (SEC) is driven by the Walker Circulation. Warm waters
 129 return eastwards via the North Equatorial Countercurrent (NECC, see Fig. 2). An abrupt transition between the cold SEC and
 130 the warm NECC is the Equatorial Front (EF, Pak and Zaneveld, 1974).

131 1.1.2 Geography, vegetation and pollen transport

132 Ecuador is geographically divided into three main regions: the coastal plain with several rivers draining into the Pacific, the
 133 Andes, and the eastern lowlands which constitute the western margin of the Amazon Basin. The mountains form two parallel
 134 cordilleras which are separated by the Interandean Valley. The diverse vegetation is the result of the combined effects of
 135 elevation and precipitation. In the coastal plain there is an abrupt shift from tropical lowland rainforests in the north to a desert
 136 dominated by annual xerophytic herbs in the south. This shift reflects the dependence of the vegetation on precipitation which
 137 ranges from 100 to 6000 mm per year on the coastal plain. The western slopes of the Andes are covered by montane forest,
 138 which is partly interrupted by drier valleys in southern Ecuador (Balslev, 1988).

139 Along the coast, mangrove stands occur in the salt- and brackish-water tidal zone of river estuaries and bays. They are formed
 140 by two species of *Rhizophora* (*R. harrisonii* and *R. mangle*), and to a lesser extent *Avicennia*, *Laguncularia*, and *Conocarpus*
 141 are present (Twilley et al., 2001). The lowland rainforest is characterized by the dominant plant families Fabaceae, Rubiaceae,
 142 Arecaceae, Annonaceae, Melastomataceae, Sapotaceae, and Clusiaceae in terms of species richness. In the understory,
 143 Rubiaceae, Araceae, and Piperaceae form the predominant elements (Gentry, 1986). In the lower montane forest, *Cyathea*,
 144 Meliaceae (e.g. *Ruagea*), Fabaceae (e.g. *Dussia*), Melastomataceae (e.g. *Meriania*, *Phainantha*), Rubiaceae (e.g. *Cinchona*),
 145 Proteaceae (e.g. *Roupala*), Lauraceae (e.g. *Nectandra*), and Pteridaceae (e.g. *Pterozonium*) are common elements. Upper
 146 montane forests are dominated by *Myrsine*, *Ilex*, *Weinmannia*, *Clusia*, *Schefflera*, *Myrcianthes*, *Hedyosmum*, and *Oreopanax*

147 (Jørgensen and León-Yáñez, 1999). Above ca. 3200 m, trees become sparse and eventually the vegetation turns into páramo.
148 The páramo is a unique ecosystem of the high altitudes of the northern Andes of South America and of southern Central
149 America, located between the continuous forest line and the permanent snowline at about 3000–5000 m (Luteyn, 1999). The
150 grass páramo is formed by tussock grasses, mainly *Calamagrostis* and *Festuca*. These are complemented by shrubs of
151 *Diplostegium*, *Hypericum*, and *Pentacalia*, and forest patches of *Polylepis*. The shrub páramo consists of cushion plants like
152 *Azorella*, *Plantago*, and *Werneria*, and shrubs like *Loricaria* and *Chuquiraga*. The vegetation of the desert páramo is scarce.
153 Some common taxa are *Nototriche*, *Draba*, and *Culcitium* (Sklenár and Jørgensen, 1999).
154 Ríncon-Martínez et al. (2010) showed that the terrigenous sediment supply at ODP Site 1239 during Pleistocene interglacials
155 is mainly fluvial and input of terrestrial material drops to low amounts during the drier glacial stages. Consequently, transport
156 of pollen and spores to the ocean is also mainly fluvial (González et al., 2010). High rates of orographic precipitation
157 characterize the western part of equatorial South America. These heavy rains quickly wash out any pollen that might be in the
158 air and result in large discharge by the Ecuadorian Rivers (Fig. 2). Esmeraldas and Santiago Rivers mainly drain the northern
159 coastal plain of Ecuador, and the southern coastal plain is drained by several smaller rivers, which end in the Guayas River
160 (Balslev, 1988). Moreover, the predominantly westerly winds (Fig. 2) are not favorable for eolian pollen dispersal to the ocean.
161 Nevertheless, some transport by SE trade winds is possible and should be taken into account.
162 After reaching the ocean, pollen and spores might pass the Peru-Chile Trench – which is quite narrow along the Carnegie
163 Ridge – by means of nepheloid layers at subsurface depths. Some northward transport from the Bay of Guayaquil by the
164 Coastal Current (Fig. 2) is likely. However, the Peru-Chile Current flows too far from the coast to have strong influence on
165 pollen and spore dispersal. We consider western Ecuador, northernmost Peru and southwestern Colombia the main source
166 areas of pollen and spores in sediments of ODP Site 1239.

167 **1.1.3 Drilling site**

168 ODP Site 1239 is located at 0°40.32'S, 82°4.86'W, about 120 km offshore Ecuador in a water depth of 1414m, near the eastern
169 crest of Carnegie Ridge and just next to a downward slope into the Peru-Chile Trench (Mix et al., 2003). Its location is close
170 to the Equatorial Front (Fig. 2) which separates the warm and low-salinity waters of Panama Basin from the cooler and high-
171 salinity surface waters of the EEP CT. The region of Site 1239 reveals a thick sediment cover, with dominant sediments in the
172 region being foraminifer-bearing diatom nannofossil ooze (Mix et al., 2003). A tectonic backtrack path on the Nazca plate
173 (Pisias, 1995) reveals a paleoposition of Site 1239 about 150–200 km further westward (away from the continent) and slightly
174 southward relative to South America at 4–5 Ma compared to the present day position (Mix et al., 2003). Due to its proximity
175 to the Ecuadorian coast, Site 1239 is suitable to record changes in fluvial runoff, related to variations of precipitation in
176 northwestern South America. Most of the material is discharged by the Guayas River and Esmeraldas River (Rincón-Martínez
177 et al., 2010).

178

180 **Table 1. List of identified pollen and spore taxa in marine ODP Holes 1239A (Pliocene samples) and 1239B (core top**
 181 **samples, taxa in grey occurred only in core top samples) and grouping according to their main ecological affinity**
 182 **(Flantua et al., 2014; Marchant et al., 2002).**
 183

Páramo	Upper montane forest	Lower montane forest	Lowland rainforest	Broad range taxa	Humid indicators
<i>Polylepis/Acaena</i>	Podocarpaceae	Urticaceae/ Moraceae	<i>Wettinia</i>	Poaceae	Cyperaceae
<i>Jamesonia/Eriosorus</i>	<i>Hedyosmum</i>	<i>Erythrina</i>	<i>Socratea</i>	Cyperaceae	<i>Ranunculus</i>
<i>Huperzia</i>	<i>Clethra</i>	<i>Alchornea</i>	Polypodiaceae	Tubuliflorae (Asteraceae)	<i>Hedyosmum</i>
<i>Ranunculus</i>	<i>Morella</i>	<i>Styloceras T</i>	<i>Pityrogramma/ Pteris altissima T</i>	Amaranthaceae	<i>Ilex</i>
<i>Draba</i>	Acanthaceae	Malpighiaceae		Rosaceae	<i>Pachira</i>
<i>Sisyrinchium</i>	Melastomataceae	Cyatheaceae		<i>Ambrosia/ Xanthium</i>	<i>Morella</i>
<i>Cystopteris diaphana T</i>	<i>Daphnopsis</i>	<i>Vernonia T</i>		Ericaceae	Malpighiaceae
	<i>Bocconia</i>	<i>Pteris grandifolia T</i>		<i>Artemisia</i>	Cyatheaceae
	<i>Myrsine</i>	<i>Pteris podophylla T</i>		<i>Ilex</i>	<i>Selaginella</i>
	<i>Lophosoria</i>	<i>Saccoloma elegans T</i>		<i>Thevetia</i>	<i>Pityrogramma/ Pteris altissima T</i>
	<i>Elaphoglossum</i>	<i>Thelypteris</i>		<i>Salacia</i>	<i>Hymenophyllum T</i>
	<i>Hypolepis hostilis T</i>	<i>Ctenitis subincisa T</i>		Bromeliaceae	<i>Thelypteris</i>
	<i>Grammitis</i>			Malvaceae	<i>Ctenitis subincisa T</i>
	<i>Dodonaea viscosa</i>			Euphorbiaceae	<i>Alnus</i>
	<i>Alnus</i>			<i>Liliaceae</i>	<i>Cystopteris diaphana T</i>
				Lycopodiaceae excl. <i>Huperzia</i> <i>Selaginella</i>	
				<i>Hymenophyllum T</i>	
				<i>Calandrinia</i>	

184

185

186 2 Methods

187 A total of 65 samples of 10 cm³ volume have been analyzed. For the interval between 301 and 334 mbsf (4.7 and 4.2 Ma), 46
 188 sediment samples were taken at 67 cm intervals on average from ODP Hole 1239A (cores 33X5-37X1). Seventeen samples
 189 were taken more or less regularly distributed over the rest of the upper 450 m of Hole A (until 6 Ma). Additionally, two core
 190 top samples were taken from ODP Hole 1239B as modern analogues. Standard analytical methods were used to process the
 191 samples, including decalcification with HCl (~10%) and removal of silicates with HF (~40%). Two tablets of exotic
 192 *Lycopodium* spores (batch #177,745 containing 18584 ± 829 spores per tablet) were added to the samples during the
 193 decalcification step for calculation of pollen concentrations (grains/cm³). After neutralization with KOH (40%) and washing,
 194 the samples were sieved with ultrasound over an 8µm screen to remove smaller particles. Samples were mounted in glycerin

195 and a minimum of 100 pollen/spore grains (178 on average, Fig. S1) were counted in each sample using a Zeiss Axioskop and
196 400x and 1000x (oil immersion) magnification.

197 For pollen identification, the Neotropical Pollen Database (Bush and Weng, 2007), a reference collection for Neotropical
198 species held at the Department of Palynology and Climate Dynamics in Göttingen, and related literature (Colinvaux et al.,
199 1999; Hooghiemstra, 1984; Murillo and Bless, 1974, 1978; Roubik and Moreno, 1991) were used. Pollen types were grouped
200 according to their main ecological affinity (Flantua et al., 2014; Marchant et al., 2002). The zonation of the diagrams was
201 based on constrained cluster analysis by sum-of-squares (CONISS) of the pollen percentage curves, using the square root
202 transformation method (Edwards & Cavalli-Sforza's chord distance) implemented in TILIA (Grimm, 1991, Supplementary
203 Figure). Percentages are based on the pollen sum, which includes all pollen and fern spore types including unidentifiable ones.
204 Confidence intervals were calculated after Maher (1972). An initial age model for Site 1239 was established based on
205 biostratigraphic information (Mix et al., 2003). The age model was refined by matching the benthic stable isotope records from
206 Site 1239 with those from Site 1241 by visual identification of isotope stages (Tiedemann et al., 2007). Site 1241 has an
207 orbitally tuned age model. Thus, this procedure resulted in an indirectly orbitally tuned age model for Site 1239, spanning the
208 interval from 5 to 2.7 Ma (Tiedemann et al., 2007, Fig. S2). A coring gap of ca. 5 meters exists between cores 35X (347 mcd)
209 and 36X (352 mcd) of Hole 1239A (Tiedemann et al., 2007; Table AT3).

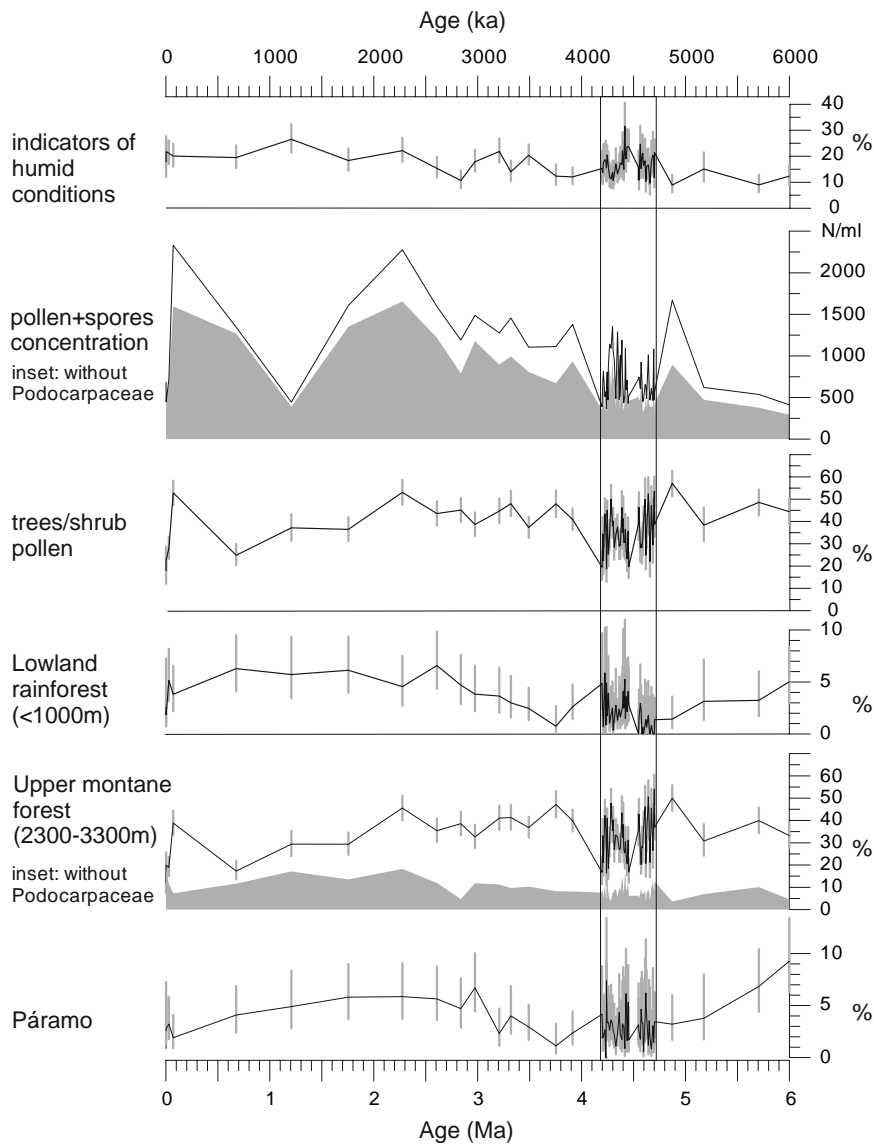
210 Elemental concentrations (total elemental counts) of Fe and K were measured in high resolution (every 2 cm) using an
211 Avaatech™ X-Ray Fluorescence (XRF) Core Scanner at the Alfred-Wegener-Institute, Bremerhaven, with correction for dead
212 time. Both Holes A and B of ODP Site 1239 were sampled. A nondestructive measuring technique was applied, allowing rapid
213 semi-quantitative geochemical analysis of sediment cores (Richter et al., 2006). Several studies comparing XRF core scanner
214 data to geochemical measurements on discrete samples showed that major elements can be precisely measured with the scanner
215 in a non-destructive way (e.g. Tjallingii et al., 2007).

216 **3 Results**

217 Five groups were established with pollen taxa grouped according to their main ecological affinity (Table 1). The groups
218 páramo, upper montane forest, lower montane forest, and lowland rainforest represent vegetation belts with different altitudinal
219 ranges (Hooghiemstra, 1984; Van der Hammen, 1974). To track changes of humidity, an additional group named "Indicators
220 of humid conditions" was established. This group includes those taxa that permanently need humid conditions to grow.
221 Changes of the pollen percentages of the ecological groups for the Pliocene interval and the core top samples are shown in
222 Figs. 3 and 5. Pollen percentages of single taxa are shown in Fig. S1.

223 To put the results of the detailed early Pliocene section into context of long-term changes, we plot a selection together with
224 the results of a coarse resolution pilot study in Fig. 3. Percentages of humidity indicators hint to slightly drier conditions at the
225 beginning of the Pliocene. A trend towards higher palynomorph concentrations is found for the period from 6 to 2 Ma. Grass
226 pollen percentages remain low indicating mainly closed forest at altitudes below the páramo. Representation of lowland
227 rainforest was low around 4.7 Ma, increased by 4.5 Ma, declined again to low levels around 3.5 Ma, and rose to remain at
228 higher levels during the Pleistocene. Continuous presence of pollen and spores from the páramo indicates that the Ecuadorian
229 Andes had reached high altitudes before the Pliocene.

230

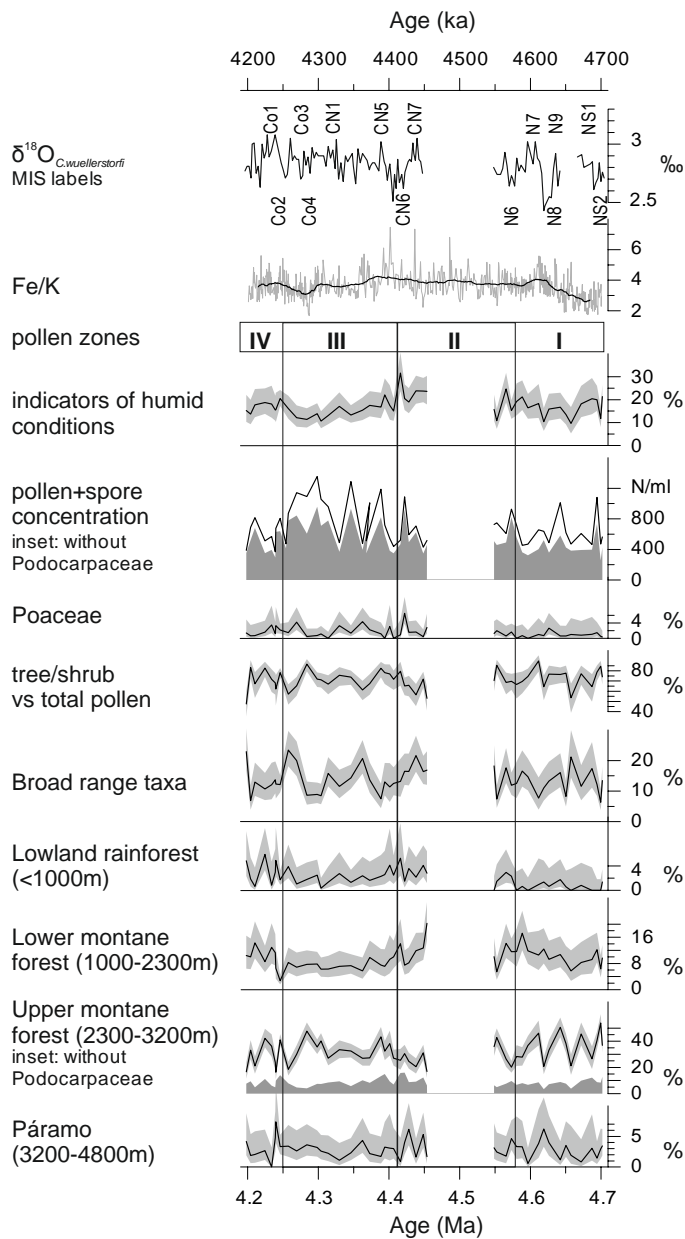


231

232 **Figure 3. Pliocene and Pleistocene palynomorph percentages (based on the total of pollen and spores) of ODP Hole 1239A for three**
 233 **vegetation belts, humidity indicators, grass pollen and pollen and spore concentration per ml. 95% confidence intervals as grey bars**
 234 **after Maher (1972). Age model for the last 5 Ma after Tiedemann et al. (2007) and for 6 to 5 Ma after Mix et al. (2003).**

235 **3.1 Description of the early Pliocene pollen record**

236 In the early Pliocene samples, 141 different palynomorph types were recognized, including 77 pollen and 64 fern spore types.
 237 A high percentage of tree and shrub pollen (46–88%) is present throughout the interval, compared to low percentages of herbs
 238 and grass pollen (0–25%; Fig. 4). In most of the vegetation belts, one or two pollen or spore taxa are overrepresented. The
 239 lowland rainforest is mainly represented by Polypodiaceae, the lower montane forest is controlled by Cyatheaceae, and the
 240 upper montane forest is strongly influenced by Podocarpaceae and *Hedyosmum*. In the páramo, the percentages of the pollen
 241 taxa are more evenly balanced. Of the total sum, the Andean forest pollen makes by far the largest percentage, with the upper
 242 montane forest ranging between 17 and 54% and the lower montane forest between 5 and 19%. The páramo is represented
 243 with 0 to 10% and the lowland rainforest with 0 to 6%. The remaining fraction has a wide or unknown ecological range.
 244



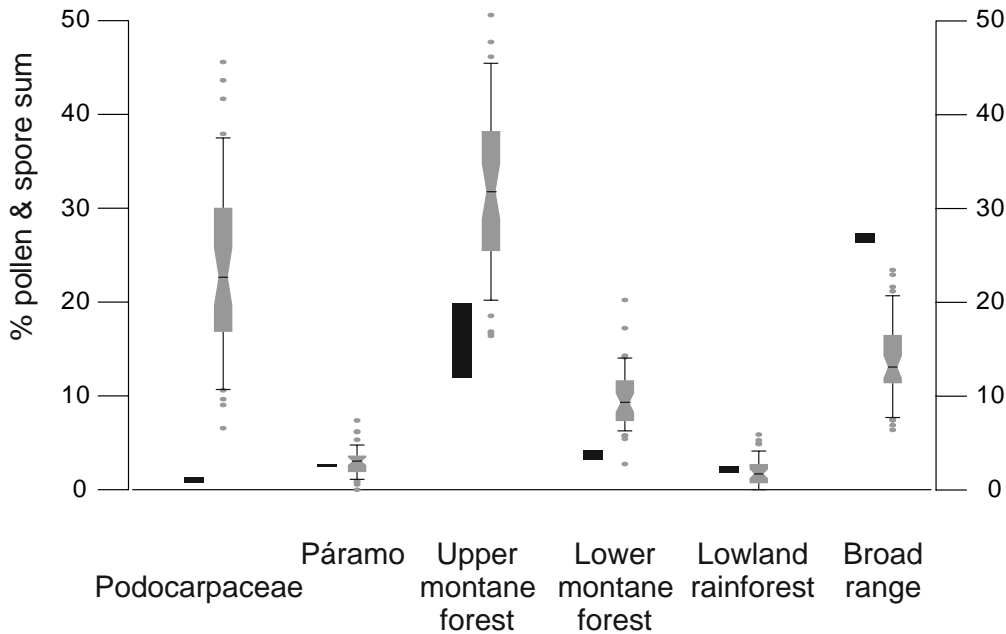
245

246 **Figure 4. Palynomorph percentages of ODP Hole 1239A for the four vegetation belts and other groups from 4.7 to 4.2 Ma. Grey**
 247 **shading represents the 95% confidence intervals (after Maher, 1972). Vertical black lines delimit the pollen zones. At the top stable**
 248 **oxygen isotopes of the benthic foraminifer *C. wuellerstorfi* (Tiedemann et al., 2007) of ODP Hole 1239A, marine isotope stages (MIS),**
 249 **and elemental ratios of Fe/K from Holes 1239A and 1239B. Ages are from Tiedemann et al. (2007). A coring gap is present in Hole**
 250 **1239A between 4.45 and 4.55 Ma.**

251

252 The pollen record of ODP Hole 1239A was divided into four main pollen zones based on constrained cluster analysis (Fig. 4
 253 and Fig. S1). Pollen zone I (333.4–325.2 mbsf: 4.70–4.58 Ma, 14 samples) has low pollen and spores concentrations. It is
 254 characterized by low pollen percentages of lowland rainforest, increases in pollen values of lower montane forest, the
 255 percentage of fern spores, and the Fe/K ratio. The pollen concentrations of broad range taxa, upper montane forest, páramo,
 256 and indicators of humid conditions go through frequent fluctuations. Coastal desert herbs (Amaranthaceae) are well represented
 257 (Fig. S1). Percentages of Poaceae pollen are low. In pollen zone II (324.8–316.4 mbsf: 4.46–4.42 Ma, 10 samples), the pollen
 258 and spores concentration is similar to pollen zone I. The lowland rainforest pollen, indicators of humid conditions, and the
 259 Fe/K ratio reach their maximum. Fern spores also reach their first maximum. Percentages of lower montane forest and páramo
 260 are high, whereas the percentage of upper montane forest is low at this time due to a strong decline of Podocarpaceae pollen.
 261 The representation of broad range taxa diminish in the interval above the gap, the decrease being mainly controlled by
 262 *Selaginella*, *Cyperaceae*, *Ambrosia/Xanthium*, and *Amaranthaceae*. Pollen zone II encloses a coring gap of almost 100 ka.
 263 Pollen zone III (315.5–305.4 mbsf: 4.41–4.26 Ma, 14 samples) shows a stepwise increase of the pollen and spores

264 concentration with its maximum at 4.3 Ma. The concentration is strongly controlled by Podocarpaceae pollen which account
 265 for up to 44% in this zone. The pollen of lowland rainforest, lower montane forest, páramo, indicators of humid conditions,
 266 and Fe/K show lower values than in zone II. Broad range taxa show some larger fluctuations. The upper montane forest pollen
 267 has its maximum extent of this zone (48%) at 4.28 Ma due to the high percentage of Podocarpaceae. If the Podocarpaceae
 268 pollen are excluded from the upper montane forest, the representation of this vegetation belt shows the same pattern of decline
 269 as that of the lower montane forest and lowland rainforest. In pollen zone IV (304.7–301.3 mbsf: 4.25–4.12 Ma, 8 samples),
 270 the pollen and spores concentration decreases sharply after 4.24 Ma. The pollen percentage of lower montane forest increases.
 271 The percentage of fern spores is at its maximum in this zone. Percentages of páramo, upper montane forest, broad range taxa,
 272 indicators of humid conditions, and the Fe/K ratio remain similar as in zone III. The percentage of lowland rainforest pollen
 273 goes through frequent and large fluctuations.



274
 275 **Figure 5. Comparison of the palynomorph percentages (based on total pollen and spores) of Podocarpaceae and the different**
 276 **vegetation belts between 2 Holocene samples (black) and Pliocene samples between 4.7-4.2 Ma (box-whisker plots).**

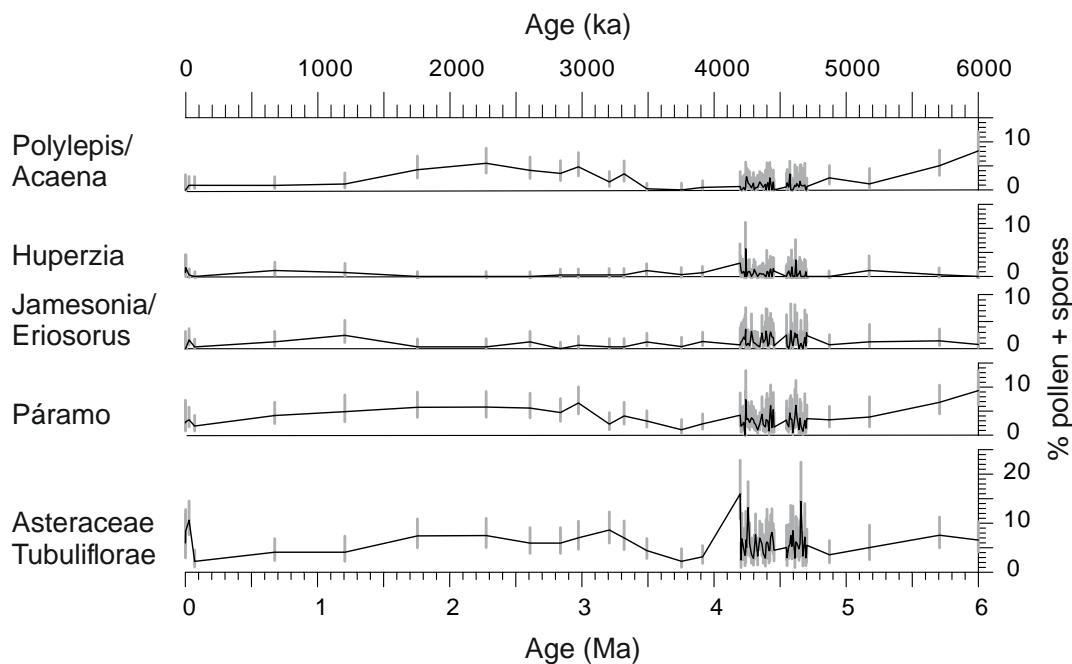
277

278 3.2 Modern vs. Pliocene pollen assemblages

279 Two samples from the top of ODP Hole 1239B have been analyzed to facilitate a comparison of the recent palynological signal
 280 with modern vegetation (Fig. 5 and Fig. S1). Although there is no detailed age control on these surface/subsurface samples, a
 281 Holocene age can be assigned based on the benthic oxygen isotope record (Rincón-Martínez et al., 2010). Fifty-one different
 282 palynomorph types were recognized, including 29 pollen and 22 fern spore types. The samples are characterized by low pollen
 283 and spore concentrations of 685 and 465 grains/cm³, respectively. Indicators of humid conditions show intermediate values.
 284 Herbs and grass pollen are very abundant with 20–26%, but tree and shrub pollen decreased to 35–46% compared to the early
 285 Pliocene interval. Broad range taxa reach their maximum abundance with 26–27%. Lowland rainforest and páramo pollen
 286 have similar representations as in the Pliocene, whereas the lower and upper montane forest pollen reach their lowest
 287 percentages. When compared to the Pliocene pollen composition, some floristic differences are seen. During the Holocene
 288 *Podocarpus* is replaced by *Alnus* as the most abundant upper montane forest tree, although *Podocarpus* was still abundant
 289 during the glacial (González et al. 2010). Another notable difference is the presence of *Rhizophora* pollen in one of the core
 290 top samples, whereas it is completely absent in the early Pliocene interval.

291 **3.3 Description of the páramo**

292 The pollen spectrum from the páramo at ODP Site 1239 includes three different taxa which are mainly confined to the páramo:
293 the pollen type *Polylepis/Acaena*, and the fern spores *Huperzia* and *Jamesonia/Eriosorus* (Fig. 6). Other taxa, which are
294 characteristic of páramos but cannot be exclusively attributed to this ecosystem, were not included in the páramo sum (e.g.
295 Asteraceae, Poaceae, Ericaceae). The record shows the continuous presence of páramo vegetation since at least 6 Ma. The
296 summed páramo pollen constitutes up to 9% of the total pollen and spore sum, with the highest fraction found at the beginning
297 of the record (6 Ma), and the lowest fractions around 4.23 and 4.59 Ma, at ca. 3.75 Ma and during the late Pleistocene (Figs.
298 4 and 6).
299



300
301 **Figure 6. Palynomorph percentages of páramo indicators and Asteraceae Tubuliflorae (excluding *Ambrosia/Xanthium* T) of the past**
302 **6 Ma indicating the presence of páramo vegetation at least since the late Miocene. 95% confidence intervals (grey bars) after Maher**
303 **(1972). Ages after Tiedemann et al. (2007) and Mix et al (2003).**

304

305 **4 Discussion**

306 **4.1 Fe/K as a tracer for changes in fluvial runoff**

307 The Fe/K ratio has been shown to be a suitable tracer to distinguish between terrigenous input of slightly weathered material
308 from drier regions and highly weathered material from humid tropical latitudes. Sediments from deeply chemically weathered
309 terrains have higher iron concentrations compared to the more mobile potassium (Mulitza et al., 2008). Before paleoclimatic
310 interpretations can be made based on elemental ratios, other processes which possibly influence the distribution of Fe/K in
311 marine sediments should be examined, like changes of the topography of Andean river drainage basins, the input of mafic rock
312 material, or diagenetic Fe remobilization (Govin et al., 2012). For northeastern South America it was shown that during the
313 middle Miocene, uplift of the Eastern Andean Cordillera led to changes in the drainage direction of the Orinoco and Magdalena
314 rivers and to the formation of the Amazon River (Hoorn, 1995; Hoorn et al., 2010). If a similar temporal history of uplift and
315 changing drainage patterns is assumed for the western Andean Cordillera, the large-scale patterns of the present topography
316 and river drainage basins should have been in place by the early Pliocene. Therefore, the main direction of fluvial transport of
317 Fe should have been similar to today. Diagenetic alteration was shown not to affect Fe concentrations at Site 1239 (Rincón-
318 Martínez, 2013). The Fe/K ratio therefore seems to be an adequate tracer of fluvial input at this study site. The trend of Fe/K

319 is similar to the pattern of humidity inferred from the pollen spectrum, showing the highest values around 4.46 Ma, thus
320 supporting the hydrological interpretation of the pollen record.

321 **4.2 The Holocene as modern reference**

322 In order to better understand the source areas and transport ways of pollen grains to the sediments, we make a comparison of
323 the results of our two Holocene samples (Fig. S1) with that of another pollen record retrieved from the Carnegie Ridge
324 southeast of ODP Site 1239 (TR 163-38, Fig. 2) reflecting rainfall and humidity variation of the late Pleistocene (González et
325 al. 2006). Holocene samples of Site 1239 gave similar results showing extensive open vegetation (indicated by pollen of
326 Poaceae, Cyperaceae, Asteraceae) and maximum relative abundance of fern spores although concentration is low (González
327 et al., 2006). As also indicated by the elemental ratios, fluvial transport of pollen predominates in this area (González et al.,
328 2006; Ríncon-Martínez, 2013). This is understandable, as both ocean currents and wind field do not favor transport from
329 Ecuador to Site 1239 (Fig. 2).

330 Despite the expansion of open vegetation, González et al. (2006) interpreted this record to reflect permanently humid
331 conditions, with disturbance processes caused by human occupation and more intense fluvial dynamics. The relatively high
332 percentage of indicators of humid conditions in our core top samples compared to pollen zones III and IV in the early Pliocene
333 would be in agreement with this interpretation. The core top samples from ODP hole 1239B and the most recent part of core
334 TR 163-38 are taken as a basis for the hydrological interpretation of the Pliocene pollen record.

335 **4.3 Climatic implications of vegetation change**

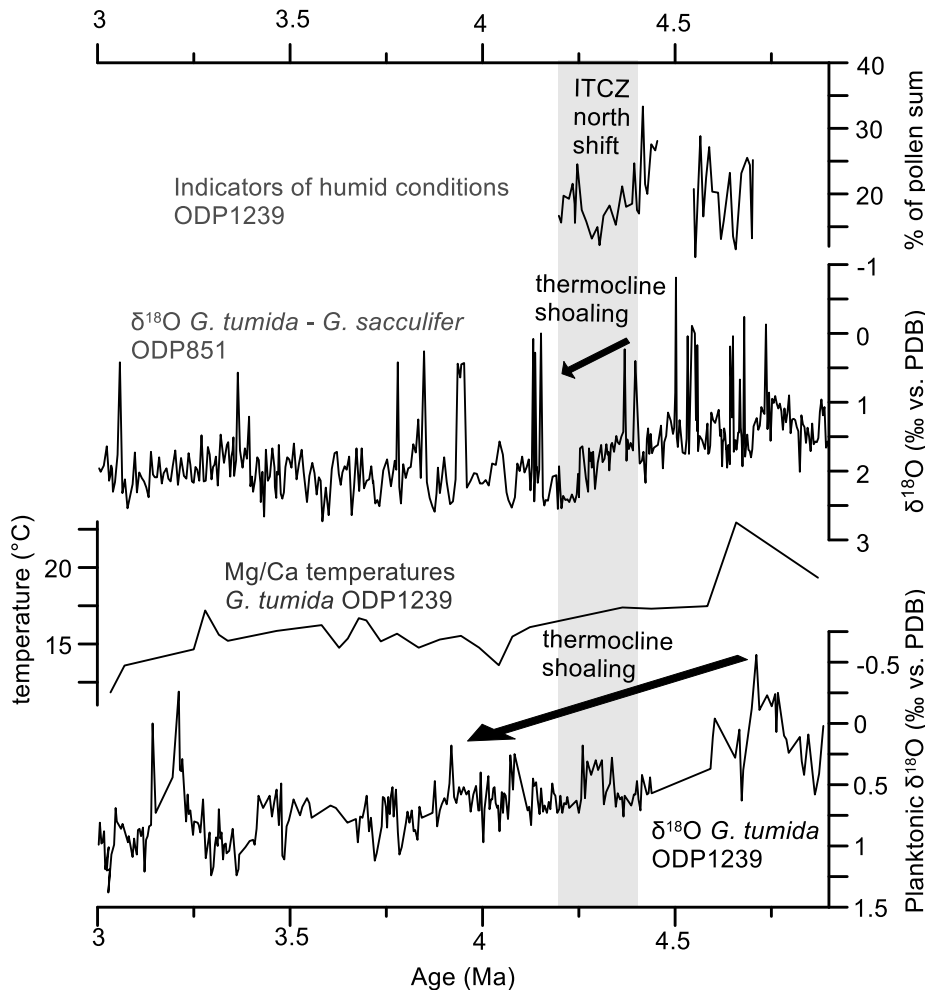
336 The presented marine palynological record provides new information on floristic and vegetation changes occurring along
337 diverse ecological and climatic gradients through the early Pliocene. The consistently high percentage of tree and shrub pollen,
338 compared to a low percentage of herbs and grass pollen (< 25%) suggests the predominance of forests and the nearly absence
339 of open grasslands (apart from páramo) during the early Pliocene. Moreover, the very low percentage of dry indicators
340 (Amaranthaceae) suggests the absence of persisting drought conditions and supports the idea of a rather stable and humid
341 climate that favored a closed forest cover. This is in good accordance with Pliocene climate models suggesting warmer and
342 wetter conditions on most continents, which led to expansions of tropical forests and savannas at the expense of deserts, for
343 instance in Africa (Salzmann et al., 2011). During the early Pliocene, no profound changes in the vegetation occur. All
344 altitudinal vegetation belts are already present, with varying ratios, and only pollen percentages of lowland rainforest rise from
345 almost absent to 6%.

346 Shifts in the vegetation are driven by various parameters such as temperature, precipitation, CO₂, radiation, and any
347 combination thereof. However, a hint to which parameter has strongest influence on the vegetation might be given by the
348 pattern of expansion and retreat of different vegetation belts. Hooghiemstra and Ran (1994) indicate that if temperature were
349 the dominant driver of vegetation change, altitudinal shifting of vegetation belts would lead to increase in the representation
350 of one at the cost of another. We hardly see such a pattern in our record with the possible exception in zone III where the trends
351 between pollen percentages of páramo and those of upper montane forest (without Podocarpaceae) are reversed (Section 4.3.2;
352 Fig. 8). However, the more general pattern indicates parallel changes in the representation of the forest belts suggesting that
353 not temperature but humidity had the stronger effect on the Pliocene vegetation of Ecuador.

354 **4.3.1 Development of the coastal vegetation**

355 Early Pliocene pollen zones I and IV show an expansion of coastal desert herbs (Amaranthaceae, Fig. S1), which coincides
356 with low sea-surface temperatures at ODP Site 846 in the EEP, suggesting an influence of the Peru-Chile Current (continuation
357 of the Humboldt Current) on the coastal vegetation of southern Ecuador. Remarkably, the lowland rainforest and the coastal
358 desert herbs follow a similar trend. This seems odd at the first glance, but a possible mechanism to explain this pattern would

359 invoke effects of El Niño, the warm phase of ENSO. The main transport agent for pollen in this region are rivers, but in the
 360 coastal desert area of southern Ecuador and northern Peru, fluvial discharge rates are low (Milliman and Farnsworth, 2011).
 361 Therefore, pollen might be retained on land until an El Niño event causes severe flooding in the coastal areas (Rodbell et al.,
 362 1999) and episodically fills the rivers which transport the pollen to the ocean. Such possible effects of El Niño seem to be
 363 strongest in pollen zones I and IV where pollen percentages of the lowland rainforest and coastal desert herbs, but also the
 364 upper montane forest, fluctuate most strongly. The lowland rainforest of the coastal plain of Ecuador and western Colombia is
 365 within the present-day range of the ITCZ, and expanded from 4.7 Ma onwards possibly due to a southwards displacement of
 366 the mean latitude of the ITCZ (Figs. 3 and 4).
 367



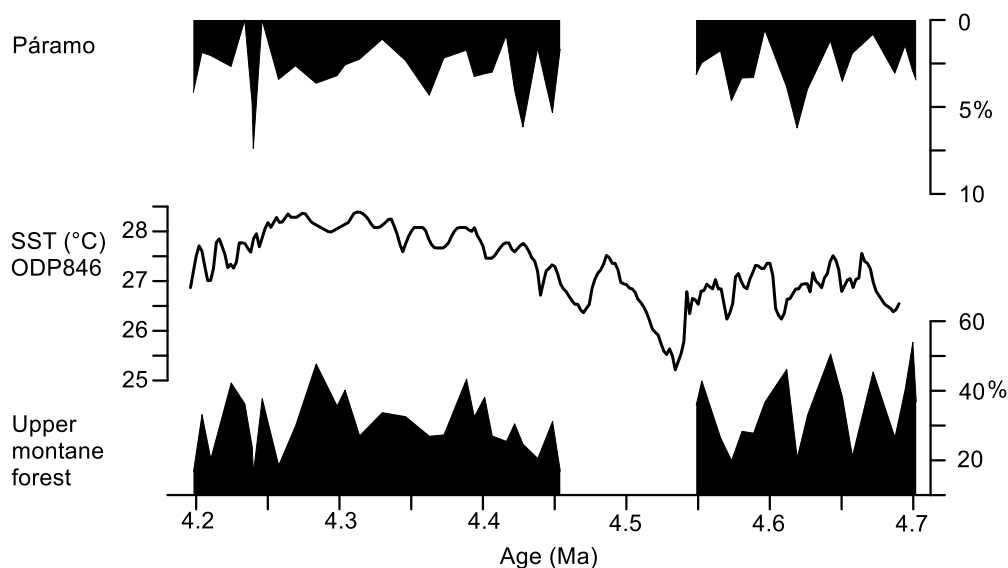
368
 369 **Figure 7.** Percentages of indicators of humid conditions (ODP Site 1239, this study), *G. tumida* – *G. sacculifer* difference in $\delta^{18}\text{O}$ from
 370 ODP Site 851 in the eastern equatorial Pacific (Cannariato and Ravelo, 1997), and *G. tumida* Mg/Ca temperatures and $\delta^{18}\text{O}$ from
 371 ODP Site 1239 (Steph, 2005; Steph et al., 2010). Grey shading marks the period of thermocline shoaling at ODP Site 851 and ITCZ
 372 north shift.

373
 374 **4.3.2 Development of the montane vegetation**

375 Podocarpaceae strongly dominate the pollen spectrum in general. However, the trend in pollen percentages of Podocarpaceae
 376 divert from that of the other pollen taxa, which may be explained by additional transport of Podocarpaceae pollen by wind.
 377 The high pollen production of Podocarpaceae and their specialized morphology (Regal, 1982) facilitate their eolian transport.
 378 In contrast, pollen from most other taxa is predominantly fluvially transported (González et al., 2006), therefore exhibiting a
 379 different pattern where high pollen concentrations correspond to high fluvial discharge in the source area. Eolian transport of
 380 Podocarpaceae explains the high pollen concentrations in pollen zone III, which occur despite less humid conditions compared

381 to pollen zones II and IV. The increased eolian transport at 4.63 Ma and between 4.4 and 4.25 Ma is proposed here to be the
 382 result of an intensification of the easterly trade winds. Increase in trade wind strength at 4.4 Ma would be in line with a shift
 383 in the locus of maximum opal accumulation rates in the ocean associated with a shift in nutrient availability from ODP Site
 384 850 to ODP Site 846 nearer to the continent (positions shown in Fig. 2) (Farrell et al., 1995). Dynamic modelling indicates
 385 that stronger easterlies would cause shoaling of the EEP thermocline (Zhang et al., 2012), which took place between 4.8 and
 386 4.0 Ma (Fig. 7; Steph et al., 2006a). Related to this process, a critical step of easterly trade wind intensification, indicated by
 387 increased eolian transport of Podocarpaceae pollen, occurred between 4.4 and 4.25 Ma.
 388 Comparing the pollen percentages of páramo and upper montane forest, Fig. 8 indicates that UMF maxima coincide with
 389 páramo minima and SST maxima at ODP Site 846 (Lawrence et al., 2006). This might be explained by a shift of the upper
 390 montane forest to higher altitudes at the cost of the area occupied by páramo vegetation as a result of higher atmospheric
 391 temperatures and/or increased orographic precipitation in the western Andean Cordillera caused by higher sea-surface
 392 temperatures and increased evaporation.

393



394

395 **Figure 8. Pollen percentages of upper montane forest and páramo, and UK'37 sea-surface temperatures (SST) of ODP site 846 in**
 396 **the eastern equatorial Pacific (Lawrence et al., 2006).**

397

398 4.4 Development of the páramo and implications for Andean uplift

399 In order to use the existence of páramo vegetation as an indicator for Andean elevation, the altitudinal restriction of the páramo
 400 taxa to environments above the forest line is a prerequisite. Although no taxa restricted to páramo were identified in the marine
 401 samples, or rather, they could not be identified due to the lack of genus-level morphological distinction (especially *Espeletia*
 402 from the Asteraceae and some Poaceae, e.g. *Festuca*), several taxa are mainly confined to high Andean environments. Dwarf
 403 trees of *Polylepis* typically form patches above the forest line and its natural altitudinal range is thought to occur between a
 404 lower limit which forms the transition to other forest types and up to 5000 m in Bolivia (Kessler, 2002). *Huperzia* occurs in
 405 montane forests as epiphytes and with terrestrial growth form in the páramo (Sklenár et al., 2011). *Jamesonia* and *Eriosorus*
 406 are both found in cool and wet highlands, with most species being found between 2200 and 5000 m (Sánchez-Baracaldo,
 407 2004). Asteraceae are not restricted to the páramo, but their occurrence in the montane forest and in the lowland rainforest of
 408 the Pacific coast is scarce (Behling et al., 1998). With a contribution of up to 16% of the pollen sum, their source area can be
 409 attributed mainly to the páramo. Additionally, the fluctuations are similar to the other páramo taxa (Fig. 6), which is another
 410 indication for their common source area.

411 The pollen record shows a continuous existence of páramo vegetation. During the warm Pliocene, the upper montane forest is
412 assumed to have extended to similar or even higher altitudes as today. Despite this upward expansion of the upper montane
413 forest, the páramo was still present, which implies that the western Cordillera of the Ecuadorian Andes had already gone
414 through substantial uplift by that time. Furthermore, the pollen record has a large montane signature, which would not be the
415 case if the Andes had reached less than half of their modern height by the early Pliocene (Coltorti and Ollier, 2000). The upper
416 montane forest which constitutes up to 60% of the pollen sum shows that montane habitats with the corresponding altitudinal
417 belts were already existent. These findings suggest an earlier development of the high Andean páramo ecosystem than
418 previously inferred from palynological studies of the eastern Cordillera in Colombia (Hooghiemstra et al., 2006; Van der
419 Hammen et al., 1973). This might also be an indication that the uplift history of the western Cordillera of Ecuador is temporally
420 more closely related to the uplift of the Central Andes where a major phase of uplift occurred between 10 and 6 Ma (Garziona
421 et al., 2008). In another recent palynological study, the arrival of palynomorphs from the páramo in sediments of the Amazon
422 Fan has been documented since 5.4 Ma (Hoorn et al., 2017). Since the Amazon has its westernmost source in Peru, this signal
423 might be related to the uplift of the Central Andes. These new records agree with paleoclimatic studies showing that modern
424 type precipitation patterns have likely been in place since the middle Miocene (Barnes et al., 2012; Hoorn et al., 2010;
425 Kaandorp et al., 2006), which would have required a significant orographic barrier. High Andean mountains acting as a climate
426 divide might thus go as far back as the Mid-Miocene. However, earliest evidence for a páramo vegetation is now set at latest
427 Miocene.

428 **4.5 Comparing models and proxy data**

429 Several studies have suggested the existence of a “permanent El Niño” during the Pliocene (e.g. Fedorov et al., 2006; Wara et
430 al., 2005). El Niño events are characterized by a shift in the Walker circulation, resulting in exceptionally heavy precipitation
431 particularly over the lowlands of central and southern Ecuador (Bendix and Bendix, 2006) and simultaneous below-average
432 rainfall over the northwestern slopes of the Andes (Vuille et al., 2000). A permanent El Niño-like climate state during the early
433 Pliocene would thus have involved permanently humid conditions with high rates of precipitation and fluvial discharge in the
434 lowlands. Such a climate would have favored the persistence of a broad rain forest coverage and precluded the development
435 of the desert that exists in coastal southern Ecuador today. The presented pollen record indeed indicates very humid conditions
436 and the only indicator of dry vegetation is a small percentage of Amaranthaceae pollen. The predicted pattern of expansion of
437 lowland rainforest at the cost of Andean forest during permanent El Niño is not reflected in the pollen record.

438 The hypothesis of a permanent El Niño climate state involving a reduced zonal Pacific sea-surface temperature gradient has
439 recently been questioned as sea-surface temperature reconstructions differ substantially depending on the method. Zhang et al.
440 (2014) claim that a zonal temperature gradient of ca. 3°C existed since the late Miocene and even intensified during the
441 Pliocene. Our pollen record instead indicates an influence of periodic El Niño-related variations on the coastal and montane
442 vegetation, especially between 4.7 and 4.55 Ma and between 4.26 and 4.2 Ma, recorded by strong fluctuations in the pollen
443 percentages of coastal and montane vegetation. Our record does not show increased representation of one vegetation belt at
444 the cost of another indicating that altitudinal shifts were not extensive and moisture availability might have been an important
445 driver of Pliocene vegetation change. Changes in humidity could be caused by a latitudinal displacement of the ITCZ. A
446 southward displacement of the ITCZ over both Atlantic and Pacific has been proposed as a response to stronger zonal
447 temperature and pressure gradients which developed after the restriction of the Central American Seaway and/or a weakening
448 of Southern Hemisphere temperature gradients (Billups et al., 1999). The timing of the southward shift was narrowed down to
449 4.4 to 4.3 Ma in this study, based on $\delta^{18}\text{O}$ records of planktonic foraminifera. The pollen record suggests a slightly different
450 timing, with a gradual southwards displacement of the ITCZ between 4.7 Ma and 4.42 Ma when the southernmost position
451 was reached. A less humid phase, indicated by a decrease of humid indicators, lowland rainforest pollen, lower montane forest
452 pollen, and the Fe/K ratio, followed between 4.42 and 4.26 Ma where the ITCZ presumably had a slightly more northern

453 position. This phase coincides with the shoaling of the thermocline at ODP Site 851 in the eastern equatorial Pacific
454 (Cannariato and Ravelo, 1997, Fig. 6). A southward displacement of the ITCZ during the early Pliocene would also be in
455 accordance with eolian deposition patterns in the EEP which show a latitudinal shift in eolian grain-size and eolian flux
456 between 6 and 4 Ma (Hovan, 1995). The rather small and slow changes in humidity imply that the ITCZ shift was a gradual
457 process, rather than the response to a single threshold. Just like the Central American Seaway was restricted and reopened
458 several times before its definitive closure at around 2.8 Ma (O'Dea et al., 2016), the atmospheric circulation might have adapted
459 gradually in several small steps to these tectonic changes.

460 Numerical models suggesting a northward shift of the ITCZ in response to the closure of the Central American Seaway or the
461 uplift of the northern Andes do not necessarily disagree with an early Pliocene southward shift inferred from proxy data. Both
462 events occurred gradually over several millions of years and despite recent advances in constraining these events, the timing
463 of major phases in the uplift histories are still debated. In the case of the Central American Seaway, the timing of surface water
464 restriction based on diverging salinities in the Caribbean and Pacific ocean, respectively, is well constrained and numerous
465 global oceanographic changes have been associated with it. Possibly these oceanic reorganizations did not directly trigger
466 modifications of the atmospheric circulation (Kaandorp et al., 2006; Hoorn et al., 2010), but critical periods of uplift
467 influencing atmospheric circulation might have occurred earlier. On the other hand, the respective model sensitivity
468 experiments generally only consider isolated changes in single boundary conditions (e.g. closed or open Central American
469 Seaway). Therefore, the effect of those (i.e. a northward shift of the ITCZ) might counteract the general trend of a southward
470 shift since the late Miocene due to a decrease in the hemispheric temperature gradient (e.g. Pettke et al., 2002). Additionally,
471 global coupled models exhibit uncertainties in the representation of ocean-atmosphere feedback and cloud-radiation
472 feedbacks, which are especially strong in the study region (i.e. showing a double ITCZ and an extensive EEP cold tongue (Li
473 and Xie, 2014)). This is problematic also in the light of the high sensitivity of the ITCZ position to slight shifts in the
474 atmospheric energy balance (Schneider et al., 2014). Another aspect to consider is that whereas proxy records record the
475 transient response of the climate system over a limited period of time, the mentioned model simulations rather follow the
476 overall equilibrium response than reproducing a stepwise process of environmental changes.

477 Concerning the uplift of the northern Andes, there is still a large uncertainty about the time when the Cordilleras reached their
478 current elevation. Moreover, phases of major uplift might have strongly differed regionally. Paleobotanists (e.g. Hooghiemstra
479 et al., 2006; Hoorn et al., 2010; Van der Hammen et al., 1973) and some tectonic geologists (e.g. Mora et al., 2008) argued for
480 a rapid rise of the Eastern Cordillera since 4–6 Ma, while others conclude that this is rather unlikely implying an earlier uplift
481 based on biomarker-based paleotemperatures (e.g. Anderson et al., 2015; Mora-Páez et al., 2016). Possibly the Pliocene
482 oceanic reorganizations did not directly trigger modifications of the atmospheric circulation, which probably was more or less
483 in place (Kaandorp et al., 2006; Hoorn et al., 2010). Critical periods of uplift influencing atmospheric circulation might have
484 occurred earlier (see also above). The estimates for uplift of the western Cordillera in Ecuador differ even more strongly, and
485 range from rapid exhumation around 13 and 9 Ma based on thermochronology (Spikings et al., 2005) to a recent uplift during
486 the Pliocene and Pleistocene (Coltorti and Ollier, 2000). Our pollen record from the páramo shows that the Ecuadorian Andes
487 must have already reached close to modern elevations by the early Pliocene in line with inferences of Hoorn et al. (2017) and
488 Bermúdez et al. (2015). If an early Andean uplift is assumed, the atmospheric response predicted by the model would have
489 occurred earlier, which would also be in agreement with proxy data indicating a northern position of the ITCZ during the late
490 Miocene (Hovan, 1995).

491 Overall, even if the timing and identification of major steps in the shoaling and restriction of the Central American Seaway or
492 in the uplift of the northern Andes are resolved, the critical threshold for profound changes in atmospheric circulation and
493 climate may have occurred at any time during the tectonic processes. Within the analyzed time window, large changes in
494 atmospheric circulation which have been proposed as a response to the closure of the Central American Seaway (Ravelo et al.,
495 2004) are absent.

496 **5 Conclusions**

- 497 1) Between 4.7 and 4.2 Ma, a permanently humid climate with broad rainforest coverage existed in western equatorial
498 South America. No evidence was found for a permanent El Niño-like climate state, but strong fluctuations in the
499 vegetation between 4.7 and 4.55 Ma and between 4.26 and 4.2 Ma indicate strong periodic El Niño variability at this
500 time. Hydrological changes between 4.55 and 4.26 Ma are attributed to gradual shifts of the Intertropical Convergence
501 Zone which reached its southernmost position around 4.42 Ma and shifted slightly north afterwards.
- 502 2) The most prominent shift recorded during the early Pliocene is an increase in the representation of the lowland
503 rainforest around 4.5 Ma.
- 504 3) Between 4.41 and 4.26 Ma, an increased eolian influx of Podocarpaceae pollen indicates an increased strength of the
505 easterly trade winds, which is presumably related to the shoaling of the EEP thermocline.
- 506 4) Results from proxy data and numerical modelling studies regarding the position of the ITCZ during the early Pliocene
507 are not necessarily contradictory. Considering the temporal uncertainties regarding major steps of CAS closure and
508 uplift of the northern Andes, the proposed northward shift of the ITCZ in response to these events might have occurred
509 much earlier (e.g. during the middle to late Miocene).
- 510 5) The continuous presence of páramo vegetation since 6 Ma implies that the Ecuadorian Andes had already reached an
511 elevation suitable for the development of vegetation above the upper forest line by the latest Miocene. We present
512 new paleobotanical evidence indicating an earlier development of páramo vegetation than previously suggested by
513 terrestrial paleobotanical records.

514

515 **Data availability**

516 The underlying research data are stored in PANGAEA as datasets PANGAEA.884280, PANGAEA.891294 and
517 PANGAEA.884153, which are combined in PANGAEA.884285 <<https://doi.pangaea.de/10.1594/PANGAEA.884285>>.

518

519 **Author contribution**

520 L. Dupont and F. Grimmer conceived the idea, and L. Dupont, F. Grimmer and F. Lamy carried out the analyses. F. Grimmer
521 prepared the manuscript with contributions from all co-authors.

522

523 **Competing interests**

524 The authors declare that they have no conflict of interest.

525

526 **Acknowledgements**

527 We thank Carina Hoorn, Jun Tian, Henry Hooghiemstra & Suzette Flantua and an anonymous referee for their insightful
528 comments on the original manuscript. This project was funded by the Deutsche Forschungsgemeinschaft (DFG) through the
529 TROPSAP project (DU221/6) and via the DFG Research Center / Cluster of Excellence “The Ocean in the Earth System —
530 MARUM”. The first author thanks GLOMAR – Bremen International Graduate School for Marine Sciences, University of
531 Bremen, Germany, for support. The IODP Gulf Coast Repository (GCR) we acknowledge for their assistance in providing the
532 core samples.

533

534 **References**

- 535 Anderson, V. J., Saylor, J. E., Shanahan, T. M., and Horton, B. K.: Paleoelevation records from lipid biomarkers:
536 Application to the tropical Andes, *Geological Society of America Bulletin*, 127, 1604-1616, 2015.
- 537 Balslev, H.: Distribution Patterns of Ecuadorean Plant-Species, *Taxon*, 37, 567-577, 1988.
- 538 Barnes, J. B., Ehlers, T. A., Insel, N., McQuarrie, N., and Poulsen, C. J.: Linking orography, climate, and exhumation
539 across the central Andes, *Geology*, 40, 1135-1138, 2012.

540 Bartoli, G., Sarnthein, M., Weinelt, M., Erlenkeuser, H., Garbe-Schönberg, D., and Lea, D. W.: Final closure of
541 Panama and the onset of northern hemisphere glaciation, *Earth and Planetary Science Letters*, 237, 33-44, 2005.

542 Behling, H., Hooghiemstra, H., and Negret, A. J.: Holocene history of the Choco Rain Forest from Laguna Piusbi,
543 Southern Pacific Lowlands of Colombia, *Quaternary Research*, 50, 300-308, 1998.

544 Bendix, A. and Bendix, J.: Heavy rainfall episodes in Ecuador during El Niño events and associated regional
545 atmospheric circulation and SST patterns, *Advances in Geosciences*, 6, 43-49, 2006.

546 Bendix, J. and Lauer, W.: Die Niederschlagsjahreszeiten in Ecuador und ihre klimadynamische Interpretation,
547 *Erdkunde*, 46, 118-134, 1992.

548 Billups, K., Ravelo, A. C., Zachos, J. C., and Norris, R. D.: Link between oceanic heat transport, thermohaline
549 circulation, and the Intertropical Convergence Zone in the early Pliocene Atlantic, *Geology*, 24, 319-322, 1999.

550 Bush, M. B. and Weng, C.: Introducing a new (freeware) tool for palynology, *Journal of Biogeography*, 34, 377-
551 380, 2007.

552 Cannariato, K. G. and Ravelo, A. C.: Pliocene-Pleistocene evolution of eastern tropical Pacific surface water
553 circulation and thermocline depth, *Paleoceanography*, 12, 805-820, 1997.

554 Colinvaux, P., De Oliveira, P. E., and Moreno Patino, J. E.: *Amazon Pollen Manual and Atlas*, Harwood Academic
555 Publishers, Amsterdam, 1999.

556 Coltorti, M. and Ollier, C. D.: Geomorphic and tectonic Evolution of the Ecuadorian Andes, *Geomorphology*, 32,
557 1-19, 2000.

558 Corredor, F.: Eastward extent of the Late Eocene-Early Oligocene onset of deformation across the northern Andes:
559 constraints from the northern portion of the Eastern Cordillera fold belt, Colombia, *Journal of South American
560 Earth Sciences*, 16, 445-457, 2003.

561 CPC Merged Analysis of Precipitation:
562 <https://www.esrl.noaa.gov/psd/data/gridded/data.ncep.reanalysis.derived.html>, last access: February 2008.

563 ETOPO1: <https://maps.ngdc.noaa.gov/viewers/wcs-client/>, last access: June 2018.

564 Fedorov, A. V., Dekens, P. S., McCarthy, M., Ravelo, A. C., deMenocal, P. B., Barreiro, M., Pacanowski, R. C., and
565 Philander, S. G.: The Pliocene paradox (mechanisms for a permanent El Niño), *Science*, 312, 1485-1489, 2006.

566 Feng and Poulsen, C. J.: Andean elevation control on tropical Pacific climate and ENSO, *Paleoceanography*, 29,
567 795–809, 2014.

568 Flantua, S., Hooghiemstra, H., Van Boxel, J. H., Cabrera, M., González-Carranza, Z., and González-Arango, C.:
569 Connectivity dynamics since the last glacial maximum in the northern Andes: a pollen-driven framework to assess
570 potential migration. In: *Paleobotany and Biogeography: A Festschrift for Alan Graham in His 80th Year*, W. D.
571 Stevens, O. M. M., P. H. Raven (Ed.), Missouri Botanical Garden Press, St. Louis, 2014.

572 Flohn, H.: A hemispheric circulation asymmetry during Late Tertiary, *Geologische Rundschau*, 70, 725-736, 1981.

573 Garziona, C. N., Hoke, G. D., Libarkin, J. C., Withers, S., MacFadden, B., Eiler, J., Ghosh, P., and Mulch, A.: Rise of
574 the Andes, *Science*, 320, 1304-1307, 2008.

575 Gentry, A. H.: Species richness and floristic composition of Chocó region plant communities, *Caldasia*, 15, 71-91,
576 1986.

577 González, C., Urrego, L. E., and Martínez, J. I.: Late Quaternary vegetation and climate change in the Panama
578 Basin: Palynological evidence from marine cores ODP 677B and TR 163-38, *Palaeogeography, Palaeoclimatology,
579 Palaeoecology*, 234, 62-80, 2006.

580 Govin, A., Holzwarth, U., Heslop, D., Ford Keeling, L., Zabel, M., Mulitza, S., Collins, J. A., and Chiessi, C. M.:
581 Distribution of major elements in Atlantic surface sediments (36°N-49°S): Imprint of terrigenous input and
582 continental weathering, *Geochemistry, Geophysics, Geosystems*, 13, 2012.

583 Gregory-Wodzicki, K. M.: Uplift history of the Central and Northern Andes: A review, *Geological Society of America
584 Bulletin*, 112, 1091-1105, 2000.

585 Grimm, E.: *Tilia and Tiliagraph*. Illinois State Museum, Springfield, 1991.

586 Groeneveld, J., Hathorne, E. C., Steinke, S., DeBey, H., Mackensen, A., and Tiedemann, R.: Glacial induced closure
587 of the Panamanian Gateway during Marine Isotope Stages (MIS) 95–100, *Earth and Planetary Science Letters*,
588 404, 296-306, 2014.

589 Haug, G. H. and Tiedemann, R.: Effect of the formation of the Isthmus of Panama on Atlantic Ocean thermohaline
590 circulation, *Nature*, 393, 673-676, 1998.

591 Haug, G. H., Tiedemann, R., Zahn, R., and Ravelo, A. C.: Role of Panama uplift on oceanic freshwater balance,
592 *Geology*, 29, 207-210, 2001.

593 Hooghiemstra, H.: *Vegetational and Climatic History of the High Plain of Bogotá, Colombia: A Continuous Record
594 of the Last 3.5 Million Years*, A.R. Gantner Verlag K.G., Vaduz, 1984.

595 Hooghiemstra, H., Wijninga, V. M., and Cleef, A. M.: The Paleobotanical Record of Colombia: Implications for
596 Biogeography and Biodiversity, *Annals of the Missouri Botanical Garden*, 93, 297-325, 2006.

597 Hoorn, C.: Andean tectonics as a cause for changing drainage patterns in Miocene northern South America,
598 *Geology*, 23, 237-240, 1995.

599 Hoorn, C., Bogotá-A., G. R., Romero-Baez, M., Lammertsma, E. I., Flantua, S., Dantas, E. L., Dino, R., do Carmo, D.
600 A., and Chemale Jr, F.: The Amazon at sea: Onset and stages of the Amazon River from a marine record, with
601 special reference to Neogene plant turnover in the drainage basin, *Global and Planetary Change*, 153, 51-65,
602 2017.

603 Hoorn, C. and Flantua, S.: An early start for the Panama land bridge, *Science*, 348, 186-187, 2015.

604 Hoorn, C., Wesselingh, F. P., ter Steege, H., Bermudez, M. A., Mora, A., Sevink, J., Sanmartin, I., Sanchez-Meseguer,
605 A., Anderson, C. L., Figueiredo, J. P., Jaramillo, C., Riff, D., Negri, F. R., Hooghiemstra, H., Lundberg, J., Stadler, T.,
606 Sarkinen, T., and Antonelli, A.: Amazonia through time: Andean uplift, climate change, landscape evolution, and
607 biodiversity, *Science*, 330, 927-931, 2010.

608 Hovan, S. A.: Late Cenozoic Atmospheric Circulation Intensity and climatic history recorded by eolian deposition
609 in the eastern equatorial pacific ocean, Leg 138, *Proceedings of the Ocean Drilling Program, Scientific Results*,
610 138, 615-625, 1995.

611 Jørgensen, P. M. and León-Yáñez, S.: Catalogue of the vascular plants of Ecuador = Catálogo de las plantas
612 vasculares del Ecuador, Missouri Botanical Garden Press, St. Louis, Missouri, 1999.

613 Kaandorp, R. J. G., Wesselingh, F. P., and Vonhof, H. B.: Ecological implications from geochemical records of
614 Miocene Western Amazonian bivalves, *Journal of South American Earth Sciences*, 21, 54-74, 2006.

615 Kessler, M.: The "Polylepis problem": Where do we stand?, *Ecotropica*, 8, 97-110, 2002.

616 Lawrence, K. T., Liu, Z., and Herbert, T. D.: Evolution of the eastern tropical Pacific through Plio-Pleistocene
617 glaciation, *Science*, 312, 79-83, 2006.

618 Li, G. and Xie, S. P.: Tropical Biases in CMIP5 Multimodel Ensemble: The Excessive Equatorial Pacific Cold Tongue
619 and Double ITCZ Problems, *Journal of Climate*, 27, 1765-1780, 2014.

620 Luteyn, J. L.: Páramos, *Memoirs of The New York Botanical Garden*, 1999.

621 Maher, L. J.: Nomograms for computing 0.95 confidence limits of pollen data, *Review of Palaeobotany and*
622 *Palynology*, 13, 85-93, 1972.

623 Marchant, R., Almeida, L., Behling, H., Berrio, J. C., Bush, M., Cleef, A., Duivenvoorden, J., Kappelle, M., De Oliveira,
624 P., Teixeira de Oliveira-Filho, A., Lozano-Garcia, S., Hooghiemstra, H., Ledru, M.-P., Ludlow-Wiechers, B.,
625 Markgraf, V., Mancini, V., Paez, M., Prieto, A., Rangel, O., and Salgado-Labouriau, M.: Distribution and ecology of
626 parent taxa of pollen lodged within the Latin American Pollen Database, *Review of Palaeobotany and Palynology*,
627 121, 1-75, 2002.

628 Marchant, R., Behling, H., Berrio, J. C., Cleef, A., Duivenvoorden, J., Hooghiemstra, H., Kuhry, P., Melief, B., Van
629 Geel, B., Van der Hammen, T., Van Reenen, G., and Wille, M.: Mid- to Late-Holocene pollen-based biome
630 reconstructions for Colombia, *Quaternary Science Reviews*, 20, 1289-1308, 2001.

631 Milliman, J. D. and Farnsworth, K. L.: *River discharge to the coastal ocean: a global synthesis*, Cambridge University
632 Press, Cambridge; New York, 2011.

633 Mix, A., Tiedemann, R., and Blum, P.: *Proceedings of the Ocean Drilling Program, Initial Reports*, 202, 2003.

634 Montes, C., Cardona, A., Jaramillo, C., Pardo, A., Silva, J. C., Valencia, V., Ayala, C., Pérez-Angel, L. C., Rondriguez-
635 Parra, L. A., Ramirez, V., and Nino, H.: Middle Miocene closure of the Central American Seaway,
636 *Paleoceanography*, 348, 226-229, 2015.

637 Mora-Páez, H., Mencin, D. J., Molnar, P., Diederix, H., Cardona-Piedrahita, L., Peláez-Gaviria, J.-R., and Corchuelo-
638 Cuervo, Y.: GPS velocities and the construction of the Eastern Cordillera of the Colombian Andes, *Geophysical*
639 *Research Letters*, 43, 8407-8416, 2016.

640 Mora, A., Parra, M., Strecker, M. R., Sobel, E. R., Hooghiemstra, H., Torres, V., and Jaramillo, J. V.: Climatic forcing
641 of asymmetric orogenic evolution in the Eastern Cordillera of Colombia, *GSA Bulletin*, 120, 930-949, 2008.

642 Mulitza, S., Prange, M., Stuetz, J. B., Zabel, M., von Döbenek, T., Itambi, A. C., Nizou, J., Schulz, M., and Wefer, G.:
643 Sahel megadroughts triggered by glacial slowdowns of Atlantic meridional overturning, *Paleoceanography*, 23,
644 2008.

645 Murillo, M. T. and Bless, M. J. M.: Spores of recent Colombian Pteridophyta. I. Trilete Spores, *Review of*
646 *Palaeobotany and Palynology*, 18, 223-269, 1974.

647 Murillo, M. T. and Bless, M. J. M.: Spores of recent Colombian Pteridophyta. II. Monolete Spores, *Review of*
648 *Palaeobotany and Palynology*, 25, 319-365, 1978.

649 NCEP reanalysis data provided by the NOAA/OAR/ESRL PSD, B., Colorado, USA:
650 <http://www.esrl.noaa.gov/psd/data/gridded/data.ncep.reanalysis.derived.html> last access: January 2010.

651 Niemann, H., Brunschön, C., and Behling, H.: Vegetation/modern pollen rain relationship along an altitudinal
652 transect between 1920 and 3185ma.s.l. in the Podocarpus National Park region, southeastern Ecuadorian Andes,
653 *Review of Palaeobotany and Palynology*, 159, 69-80, 2010.

654 NODC (Levitus) World Ocean Atlas: <http://www.esrl.noaa.gov/psd/data/gridded/data.nodc.woa94.html>, last
655 access: March 2010, 1994.

656 O’Dea, A., Lessios, A. H., Coates, A. G., Eytan, R. I., Restrepo-Moreno, S. A., Cione, A. L., Collins, L. S., de Queiroz,
657 A., Farris, D. W., Norris, R. D., Stallard, R. F., Woodburne, M. O., Aguilera, O., Aubry, M.-P., Berggren, W. A., Budd,
658 A. F., Cozzuol, M. A., Coppard, S. E., Duque-Caro, H., Finnegan, S., Gasparini, G. M., Grossman, E. L., Johnson, K.
659 G., Keigwin, L. D., Knowlton, N., Leigh, E. G., Leonard-Pingel, J. S., Marko, P. B., Pyenson, N. D., Rachello-Dolmen,
660 P. G., Soibelzon, E., Soibelzon, L., Todd, J. A., Vermeij, G. J., and Jackson, J. B. C.: Formation of the Isthmus of
661 Panama, *Science Advances*, 2, 2016.

662 Pak, H. and Zaneveld, J. R.: Equatorial Front in the Eastern Pacific Ocean, *J Phys Oceanogr*, 4, 570-578, 1974.

663 Pettke, T., Halliday, A. N., and Rea, D. K.: Cenozoic evolution of Asian climate and sources of Pacific seawater Pb
664 and Nd derived from eolian dust of sediment core LL44-GPC3, *Paleoceanography*, 17, 2002.

665 Piasias, N.: Paleoceanography of the eastern equatorial Pacific during the Neogene: Synthesis of Leg 138 drilling
666 results, *Proceedings of the Ocean Drilling Program, Scientific Results*, 138, 5-21, 1995.

667 Ravelo, A. C., Andreasen, D. H., Lyle, M. W., Lyle, A. O., and Wara, M. W.: Regional climate shifts caused by gradual
668 global cooling in the Pliocene epoch, *Nature*, 429, 2004.

669 Regal, P. J.: Pollination by Wind and Animals: Ecology of Geographic Patterns, *Annual Review of Ecology and*
670 *Systematics*, 13, 497-524, 1982.

671 Richter, T. O., van der Gaast, S., Koster, B., Vaars, A., Gieles, R., de Stigter, H. C., de Haas, H., and van Weering, T.
672 C. E.: The Avaatech XRF Core Scanner: Technical description and applications to NE Atlantic sediments. In: *New*
673 *Techniques in Sediment Core Analysis*, Rothwell, R. G. (Ed.), Geological Society, London, Special Publications,
674 2006.

675 Rincón-Martínez, D.: Eastern Pacific background state and tropical South American climate history during the last
676 3 million years, 2013. *Fachbereich Geowissenschaften, Universität Bremen, Bremen*, 2013.

677 Rincón-Martínez, D., Lamy, F., Contreras, S., Leduc, G., Bard, E., Saukel, C., Blanz, T., Mackensen, A., and
678 Tiedemann, R.: More humid interglacials in Ecuador during the past 500 kyr linked to latitudinal shifts of the
679 equatorial front and the Intertropical Convergence Zone in the eastern tropical Pacific, *Paleoceanography*, 25,
680 2010.

681 Rodbell, D. T., Seltzer, G. O., Anderson, D. M., Abbott, M. B., Enfield, D. B., and Newman, J. H.: An ~15,000-year
682 record of El Niño-driven alluviation in southwestern Ecuador, *Science*, 283, 516-520, 1999.

683 Roubik, D. W. and Moreno, P.: Pollen and spores of Barro Colorado Island, *Monographs in systematic botany from*
684 *the Missouri Botanical Garden*, 36, 1991.

685 Salzmann, U., Williams, M., Haywood, A. M., Johnson, A. L. A., Kender, S., and Zalasiewicz, J.: Climate and
686 environment of a Pliocene warm world, *Palaeogeography, Palaeoclimatology, Palaeoecology*, 309, 1-8, 2011.

687 Sánchez-Baracaldo, P.: Phylogenetics and biogeography of the neotropical fern genera *Jamesonia* and *Eriosorus*
688 (*Pteridaceae*), *American Journal of Botany*, 91, 274-284, 2004.

689 Schneider, T., Bischoff, T., and Haug, G. H.: Migrations and dynamics of the intertropical convergence zone,
690 *Nature*, 513, 45-53, 2014.

691 Seilles, B., Goni, M. F. S., Ledru, M. P., Urrego, D. H., Martinez, P., Hanquiez, V., and Schneider, R.: Holocene land-
692 sea climatic links on the equatorial Pacific coast (Bay of Guayaquil, Ecuador), *The Holocene*, 26, 567-577, 2016.

693 Sklenár, P., Dusková, E., and Balslev, H.: Tropical and Temperate: Evolutionary History of Páramo Flora, *Bot Rev*,
694 77, 71-108, 2011.

695 Sklenár, P. and Jorgensen, P. M.: Distribution patterns of Páramo Plants in Ecuador, *Journal of Biogeography*, 26,
696 681-691, 1999.

697 Spikings, R. A., Winkler, W., Hughes, R. A., and Handler, R.: Thermochronology of allochthonous terranes in
698 Ecuador: Unravelling the accretionary and post-accretionary history of the Northern Andes, *Tectonophysics*, 399,
699 195-220, 2005.

700 Steph, S.: Pliocene stratigraphy and the impact of Panama uplift on changes in Caribbean and tropical east Pacific
701 upper ocean stratification, 2005. *Mathematisch-Naturwissenschaftliche Fakultät, Christian-Albrechts-Universität*
702 *Kiel, Kiel*, 2005.

703 Steph, S., Tiedemann, R., Groeneveld, J., Sturm, A., and Nürnberg, D.: Pliocene Changes in Tropical East Pacific
704 Upper Ocean Stratification: Response to Tropical Gateways?, *Proceedings of the Ocean Drilling Program, Scientific*
705 *Results*, 202, 2006a.

706 Steph, S., Tiedemann, R., Prange, M., Groeneveld, J., Nürnberg, D., Reuning, L., Schulz, M., and Haug, G. H.:
707 Changes in Caribbean surface hydrography during the Pliocene shoaling of the Central American Seaway,
708 *Paleoceanography*, 21, 2006b.

709 Steph, S., Tiedemann, R., Prange, M., Groeneveld, J., Schulz, M., Timmermann, A., Nürnberg, D., Rühlemann, C.,
710 Saukel, C., and Haug, G. H.: Early Pliocene increase in thermohaline overturning: A precondition for the
711 development of the modern equatorial Pacific cold tongue, *Paleoceanography*, 25, 2010.

712 Takahashi, K. and Battisti, D. S.: Processes Controlling the Mean Tropical Pacific Precipitation Pattern. Part I: The
713 Andes and the Eastern Pacific ITCZ, *Journal of Climate*, 20, 3434-3451, 2007.

714 Tiedemann, R., Sturm, A., Steph, S., Lund, S. P., and Stoner, J. S.: Astronomically calibrated timescales from 6 to
715 2.5 Ma and benthic isotope stratigraphies, sites 1236, 1237, 1239, and 1241, *Proceedings of the Ocean Drilling*
716 *Program, Scientific Results*, 202, 2007.

717 Tjallingii, R., Röhl, U., Kölling, M., and Bickert, T.: Influence of the water content on X-ray fluorescence core-
718 scanning measurements in soft marine sediments, *Geochemistry, Geophysics, Geosystems*, 8, 2007.

719 Twilley, R. R., Cárdenas, W., Rivera-Monroy, V. H., Espinoza, J., Suescum, R., Armijos, M. M., and Solórzano, L.:
720 The Gulf of Guayaquil and the Guayas River Estuary, Ecuador. In: *Coastal Marine Ecosystems of Latin America*,
721 Seeliger, U. and Kjerfve, B. (Eds.), Springer, Heidelberg, 2001.

722 Van der Hammen, T.: The Pleistocene Changes of Vegetation and Climate in Tropical South America, *Journal of*
723 *Biogeography*, 1, 3-26, 1974.

724 Van der Hammen, T., Werner, J. H., and van Dommelen, H.: Palynological record of the upheaval of the Northern
725 Andes: a study of the Pliocene and Lower Quaternary of the Colombian early evolution of its high-Andean biota,
726 *Review of Palaeobotany and Palynology*, 16, 1-122, 1973.

727 Vuille, M., Bradley, R. S., and Keimig, F.: Climate variability in the Andes of Ecuador and its relation to tropical
728 Pacific and Atlantic Sea surface temperature anomalies, *Journal of Climate*, 13, 2520-2535, 2000.

729 Wara, M. W., Ravelo, A. C., and Delaney, M. L.: Permanent El Niño-like conditions during the Pliocene warm
730 period, *Science*, 309, 758-761, 2005.

731 World Wildlife Fund (WWF): <https://www.worldwildlife.org/ecoregions/> last access: October 2017.

732 Zhang, X., Prange, M., Steph, S., Butzin, M., Krebs, U., Lunt, D. J., Nisancioglu, K. H., Park, W., Schmittner, A.,
733 Schneider, B., and Schulz, M.: Changes in equatorial Pacific thermocline depth in response to Panamanian seaway
734 closure: Insights from a multi-model study, *Earth and Planetary Science Letters*, 2012. 76-84, 2012.

735 Zhang, Y. G., Pagani, M., and Liu, Z.: A 12-million-year temperature history of the tropical Pacific Ocean, *Science*,
736 344, 84-87, 2014.

737